Sugar Acetates as CO_2-philes: Molecular Interactions and Structure Aspects from Absorption Measurement Using Quartz Crystal Microbalance

Shao-Ling Ma,[†] You-Ting Wu,*[,†,‡] Michael L. Hurrey,[§] Scott L. Wallen,[§] and Christine S. Grant*[,‡]

Key Laboratory of Mesoscopic Chemistry of MOE, School of Chemistry and Chemical Engineering, Nanjing University, Nanjing, 210093, People's Republic of China, Department of Chemical Engineering, North Carolina State University, Raleigh, North Carolina 27695, and Department of Chemistry, The University of North Carolina, Chapel Hill, NC27599-3290

Received: December 30, 2009; Revised Manuscript Received: February 3, 2010

Sugar acetates, recognized as attractive CO_2-philic compounds, have potential uses as pharmaceutical excipients, controlled release agents, and surfactants for microemulsion systems in CO_2-based processes. This study focuses on the quantitative examination of absorption of high pressure CO_2 into these sugar derivatives using quartz crystal microbalance (QCM) as a detector. In addition to the absorption measurement, the QCM is initially found to be able to detect the CO_2-induced deliquescence of sugar acetates, and the CO_2 pressure at which the deliquescence happens depends on several influencing factors such as the temperature and thickness of the film. The CO_2 absorption in α-D-glucose pentaacetate (Ac-α-GLU) is revealed to be of an order of magnitude larger in comparison with its anomer Ac-β-GLU, whereas α-D-galactose pentaacetate (Ac-α-GAL) absorbs CO_2 less than Ac-α-GLU due to the steric-hindrance between the acetyl groups on the anomeric and C4 carbons, implying the significant importance of the molecular structure and configuration of sugar acetates on the absorption. The effects of molecular size and acetyl number of sugar acetates on the CO_2 absorption are evaluated and the results indicate that the conformation and packing of crystalline sugar acetate as well as the accessibility of the acetyls are also vital for the absorption of CO_2. It is additionally found that a CO_2-induced change in the structure from a crystalline system to an amorphous system results in an order of magnitude increase in CO_2 absorption. Further investigation illustrates the interaction strength between sugar acetates and CO_2 by calculating the thermodynamic parameters such as Henry's law constant, enthalpy and entropy of dissolution from the determined CO_2 absorption. Experiments and calculations demonstrate that sugar acetates exhibit high CO_2 absorption, as at least comparable to ionic liquids. Since the ionic liquids have potential uses in the separation of acidic gases, it is evident from this study that sugar acetates could be used as possible materials for CO_2 separation.

1. Introduction

Supercritical carbon dioxide ($ScCO_2$) has attracted much attention as a green replacement for organic solvents, offering economical and environmental benefits due to its favorable physical and chemical properties,[1] and has been widely used as the solvent in extraction and separation of natural products[2,3] and drugs.[4] However, many substances are insoluble or only sparingly soluble in this environmentally benign solvent due to its nondipolar nature, which challenges the applications of $scCO_2$ in this field.

Recently a class of compounds composed of sugar acetates has been recognized[5,6] to have inherent advantages over other CO_2 soluble compounds, due to its high solubility in both liquid and supercritical CO_2 under mild conditions,[6,7] together with its environmentally benign features such as biocompatible, nontoxic, nonfluorinated, and renewable. Moreover, the Lewis acid−Lewis base interactions between CO_2 and sugar acetates from spectroscopic studies[5,8] and computational calculations[9] suggest that the combination of chemistries based on a renewable chemical feedstock with the environmentally benign solvent attributes of CO_2 is a new paradigm in the development of CO_2-based applications. This includes the use of these compounds as CO_2-philic moieties for the preparation of functional surfactants for water-in-CO_2 and organic-in-CO_2 microemulsions systems,[5,10] as well as the use of CO_2 as a solvent in specialized carbohydrate synthesis, purification, and crystallization. In addition, sugar acetates show promise as a novel cosolvent and excipient system for pharmaceutical and biological applications[11,12] to reduce the excessive waste of organic solvents utilized in current pharmaceutical processing. The acetylated carbohydrate-CO_2 melt systems[13] and drug-cyclodextrin inclusion complex[12] used as pharmaceutical processing media have been reported recently.

It is also interesting that, to date, most of the CO_2-soluble sugar acetates are known to undergo deliquescence in contact with gaseous or liquid CO_2.[5] During deliquescence, a soluble or mixed soluble−insoluble solid substance adsorbs environmental vapors until a liquid film is formed. It is also found that some of the sugar acetates remain crystalline upon CO_2 processing, and others undergo an amorphous transition such that they become glasses.[11] However, the manner in which the structural aspects govern their interactions with CO_2 and the solvation of these complex materials by CO_2 is a relatively

* To whom correspondence should be addressed. E-mail: (Y.-T.W.) ytwu@nju.edu.cn; (C.S.G.) grant@eos.ncsu.edu.
[†] Nanjing University.
[‡] North Carolina State University.
[§] The University of North Carolina.

10.1021/jp9122634 © 2010 American Chemical Society
Published on Web 03/02/2010

unexplored area due to the lack of in situ tools for measurement under high pressure conditions.

The CO_2-soluble characteristics of sugar acetates also imply that CO_2 may have high solubility in these sugar derivatives. If this is the case, these compounds may have great potential to be used as materials for the separation of CO_2 from gas sources such as natural gas, flue gas, and various prepared fuel gases. Since the separation and fixation of the acidic greenhouse gas CO_2 is nowadays of great interest for the environmental protection, green materials of high CO_2 absorption are eagerly awaited. Recently, ionic liquids (ILs) have received much attention in this field due to their well CO_2 absorption capacity, as well as their green features such as nonvolatile, nonflammable, thermally, and chemical stable.[14−16] Sugar acetates with their biocompatible and renewable characteristics are also among possible selections if they can be characterized to have high performance in CO_2 absorption. In addition, both the solubility of CO_2 in sugar acetates and that of sugar acetates in CO_2 are fundamental physical properties that can be used to evaluate the interactions of sugar acetates with CO_2. Even though the solubility of sugar acetates in liquid and supercritical CO_2 has been reported,[7] little information about the absorption of CO_2 in sugar derivatives is known. Therefore, the experimental determination of the absorption of CO_2 in these sugar derivatives is of critical importance.

The high mass sensitivity to nanogram (ng) levels of piezoelectric quartz crystal microbalances (QCM) has led to increased use over the past two decades for investigations of surface films, solid-fluid interfaces, and other chemical processes.[17−20] QCMs have other advantages such as stable in situ measurements, rapid response, miniature size, simple construction,[21] and low cost. In addition, QCM is especially suitable for microweighing in high-pressure environments while conventional microbalances have difficulties in transferring gravimetric forces from the sample to the balance.[22]

Several researchers have studied the behavior of adsorption/absorption of high pressure CO_2 on/into solid films using a QCM system. The solubility of CO_2 in a variety of polymers (i.e., polycarbonate,[23] polystyrene,[24,25] polymethyl methacrylate[26]) coated on the QCM crystal surfaces at high pressures have been reported. Other compounds such as proteins,[27] polysaccharides,[27] and some complexes[28] have also been tested. All these efforts have broadened the applications of QCM in studying CO_2-base processes.

In the present study, we utilize the QCM technique as a detector to examine the absorption behavior of high-pressure CO_2 into thin films of sugar acetates coated on polished QCM crystals. Several different sugar derivatives such as α-D-glucose (α-GLU), α-D-galactose pentaacetate (Ac-α-GAL), α-D-glucose pentaacetate (Ac-α-GLU), β-D-glucose pentaacetate (Ac-β-GLU), sucrose octaacetate (SOA), α-cyclodextrin (α-CD), and peracetylated β-cyclodextrin (Ac-β-CD) were chosen to examine the influence of epimeric or anomeric configuration, overall molecular size and long-range structural order on the interactions of CO_2 with sugar acetates. An additional investigation to examine the necessary conditions (i.e., pressure and temperature) for sugar acetate deliquescence was completed. Furthermore, to determine the interaction strength of sugar acetates with CO_2, absorption data was determined to calculate the thermodynamic parameters such as Henry's law constant, enthalpy, and entropy of dissolution. The possible application of sugar acetates as separation materials of CO_2 was also evaluated by comparing them with ionic liquids, a kind of nonvolatile CO_2-philic material that are considered in current research studies for the separation of CO_2.

2. Microweighing Mechanism of QCM

The QCM microweighing technique utilizes the linear relationship between the frequency shift ΔF_m and the mass loading of foreign material Δm (g cm^{-2}) on the QCM surface, known as the Sauerbrey equation[29]

$$\Delta F_m = F - F_0 = -C_m \Delta m \quad (1)$$

where F and F_0 are the measured frequency and fundamental frequency of quartz, respectively. C_m is the mass sensitivity of the QCM, being a function of the characteristic properties of the crystal

$$C_m = \frac{2nF_0^2}{\sqrt{\mu_q \rho_q}} \quad (2)$$

where n (= 1 or 2) is the number of faces of the crystal in contact with the fluid, μ_q (= 2.947 × 10^{11} g·cm^{-1}·s^{-2}), ρ_q (= 2.648 g·cm^{-3}) are the shear modulus and density of quartz, respectively. For the QCM crystal used in this study (AT-cut, F_0 = 5.0 MHz), numerical substitution leads to C_m = 1.132 × 10^8 Hz·cm^2·g^{-1}, which means a frequency change of 1 Hz corresponds to a mass change of 8.83 ng·cm^{-2} on the crystal electrodes.

This simple correlation was originally used in vacuum,[19] but when QCM is placed under a gaseous surrounding at a certain temperature, besides the foreign mass loading Δm, the frequency shift ΔF is also affected by the pressure, density, and viscosity of the gas, as well as the surface roughness of the quartz crystal. The frequency shift caused by these effects are defined as ΔF_P, ΔF_η, ΔF_r and have the following expressions[30,31]

$$\Delta F = F - F_0 = \Delta F_m + \Delta F_P + \Delta F_\eta + \Delta F_r \quad (3)$$

$$\Delta F_P = C_P P \quad (4)$$

$$\Delta F_\eta = -0.5 C_m (\pi F_0)^{-1/2} (\rho_f \eta_f)^{1/2} \quad (5)$$

$$\Delta F_r = -0.5 C_m C_r \rho_f \quad (6)$$

where ΔF_P depends on pressure P, and the corresponding pressure sensitivity of the crystal C_P is determined by the type of fluid in contact with the crystal; ΔF_η changes with density ρ_f and viscosity η_f of the fluid; and ΔF_r is a function of surface roughness of quartz crystal, in which C_r is the frequency-roughness correlation factor, being only a function of surface roughness.[32,33] A previous study[31] pointed out that F_r could be minimized or neglected if a polished crystal with rms surface roughness less than 10 nm was used.

When a polished crystal with a chemical coating of mass M is immersed in high-pressure CO_2 environments at a given temperature and pressure, the characteristic of CO_2 (i.e., density, viscosity) are well-defined, so that ΔF_P and ΔF_η become constants according to eqs 4 and 5. In addition, since polished crystals with surface roughness less than 10 nm were used and

the same coating technology was applied to prepare chemical films of similar surface roughness on the QCM crystal, it is reasonable to assume the negligibility of the ΔF_r term.[24,31] Hence, eq 3 can be written as

$$\Delta F = F - F_0 = C + \Delta F_m \quad (7)$$

where C ($= \Delta F_P + \Delta F_\eta + \Delta F_r$) is a constant at a given temperature and pressure of CO_2. Since the total mass loading (Δm) of foreign material on the crystal is composed of mass M from the coated chemical film, mass M_A from the adsorbed CO_2 on the coated film, and mass SM from the absorbed CO_2 in the coated film, where S is the absorption of CO_2 in the film, eq 7 can be rewritten into the following final expression

$$\Delta F - \Delta F_{mf} = C - C_m(M_A + SM) \quad (8)$$

where ΔF_{mf} ($= -C_m M$) is the frequency shift due to the coated chemical film of mass M on the crystal. From eq 8, the solubility of CO_2 in the chemical film can be obtained from the slope of the plot of ($\Delta F - \Delta F_{mf}$) with respect to M.

3. Experimental Methods

3.1. Materials and Experimental Setup. Compressed CO_2 (Coleman grade, 99.99%) was purchased from National Welders, and passed through a drying column filled with granular KOH to remove water vapor before use. Ac-β-CD, Ac-β-GLU was purchased from Cerestar and Fluka respectively; other sugar derivatives such as SOA, Ac-α-GAL, Ac-α-GLU, α-CD and α-GLU were purchased from Sigma-Aldrich. Organic solvents ethyl acetate, acetone and ethanol of HPLC grade were obtained from Sigma-Aldrich. Water of extra high purity was obtained from Fisher Scientific. All the solvents and sugars were used as received without further purification.

The CO_2 absorption measurements were carried out using a QCM system. The detail of the experimental setup is described in our pervious work.[31] The CO_2 was pressurized with a syringe pump (ISCO 260D) after leaving the cylinder and drying column, then flowed through a preheating coil, and finally into the pressure cell with an internal volume of 25 cm^3 and a maximum working pressure of about 50 MPa. Both the preheating coil and the pressure cell were placed in a water bath and controlled to ±0.1 K. A pressure transducer and a thermocouple were connected to the cell to measure the pressure and temperature of fluid, respectively. The quartz crystal was mounted in the cell and connected to an oscillator circuit powered by a triple output dc supply and used to drive the crystal to reach vibration. The vibrating frequency of the crystal was displayed with a frequency counter and recorded to a computer.

An AT-cut quartz crystal (5.00 MHz) with silver electrodes sputtered on both sides were utilized in the experiments. The crystals, purchased from International Crystal Manufacturing (ICM), had the following specifications: polished crystals with an rms surface roughness of less than 5 nm, blank diameter of 8.5 mm, electrode diameter of 3.5 mm, and electrode thickness of 0.1 μm.

3.2. Experimental Methods and Procedure. Organic solutions of 1−10% w/v were prepared by weighing and mixing a known mass of solute into 20 mL of a volatile solvent. The solute and solvent pairs were as follows: α-GLU in 13:7 v/v ethanol/water solution; SOA in acetone, ethyl acetate or liquid CO_2; Ac-α-GLU in methyl acetate; Ac-α-GAL in ethyl acetate; Ac-β-GLU in acetone; α-CD in 9:11 v/v ethanol/water solution; and Ac-β-CD in ethyl acetate.

Sugar films were prepared using a dip-coating technique. A clean crystal was immersed carefully and vertically in the casting organic solution for 5 min to guarantee a stationary solution and a completely wetted crystal surface. The solution was drawn out to a storage vial with a constant-flow pump at a slow and constant speed (0.5−3 mm/s). The solution remaining on the crystal formed a thin and uniform liquid film. The crystal was kept hanging above the coating solution for another 5 min to evaporate most of the solvent on the crystal. The solid film thus obtained was completely dried in the pressure cell under vacuum condition until the frequency of the crystal was stabilized to ±1 Hz for 15 min. The sugar loading was calculated from the frequency shift (ΔF_{mf}) measured in vacuum before and after coating. The surface roughness of the crystal with or without sugar films were characterized using a Digital Instruments D3000 AFM with a Nanosope III controller and extender module.

Sugar films cast from organic solutions were all considered to be crystalline based upon previous results.[11] If a liquid CO_2 solution was applied, amorphous films were formed by free meniscus coating. These coatings were accomplished by placing a clean QCM crystal in a high-pressure, free meniscus coating cell developed in the Kenan Center for the Utilization of CO_2 in Manufacturing and the relative coating procedure was similar to that described in a recent publication by Novick, et al.[34] Briefly, 10 wt % sugar acetate solutions were prepared under high-pressure conditions in a mixing vessel and then introduced into the coating cell. After equilibration for 30 min, the CO_2 solution was displaced by injecting CO_2 vapor at a rate of 0.2 cm/s and then slowly depressurized using a back pressure regulator with an evaporation driving force of 0.04 MPa.

Once coated, each QCM was placed in a pressure cell, and the CO_2 was injected into the vessel and maintained at a specific pressure and temperature to measure the frequency shift data ΔF. The frequency of the coated crystal at the given pressure was continually monitored every 5 s until steady state was reached. Steady state is defined as the point at which a change in frequency is observed to be less than ±1 Hz over a long time scale (i.e., 15 min), noting that 1 Hz of frequency is assumed to be the resolution of the QCM technique. The time to attain this condition was typically within 20 min. The frequency shift at a given pressure and temperature, $\Delta F(= F - F_0)$, was calculated from the frequency value at steady state, F. A series of ΔF data with respect to pressure was obtained by exposing the coated QCM to several pressures of CO_2. Five films of different coated sugar masses were prepared for the determination of CO_2 absorption, the frequency shifts were then plotted as a function of film thickness for each pressure and the slope was determined.

After measurement, crystals were cleaned by immersing the crystal in a series of pure solvents and applying ultrasonic vibration. If the fundamental frequency F_0 of the crystal was not recovered after cleaning with the pure casting solvent, other organic solvents (i.e., those mentioned in Section 3.1) and double distilled water were used. In rare cases, an aqueous solution of 2% H_2O_2 was used for F_0 recovery.

4. Results and Discussion

Sugar acetates are soluble materials in high pressure CO_2 and have attractive interactions with CO_2, as evidenced from the literature.[6,7] The purpose of this paper is to investigate experimentally the interactions and absorption of CO_2 in sugar

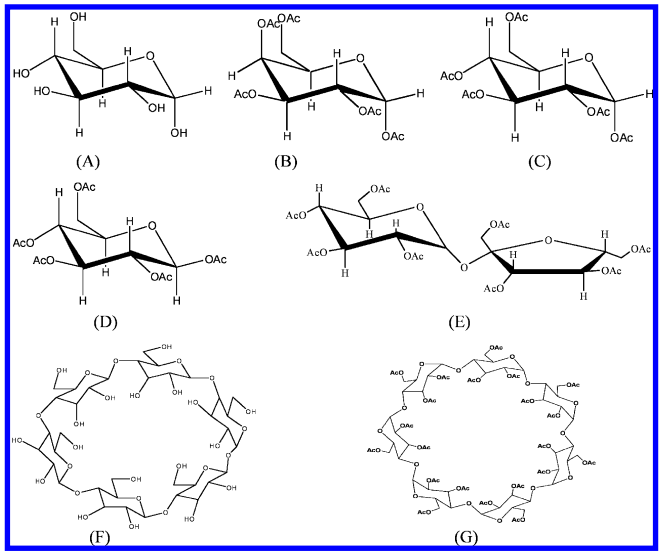

Figure 1. Sugar derivatives tested for CO_2 absorption (A) α-D-GLU, (B) Ac-α-D-GAL, (C) Ac-α-D-GLU, (D) Ac-β-D-GLU, (E) SOA, (F) α-CD, (G) Ac-β-CD.

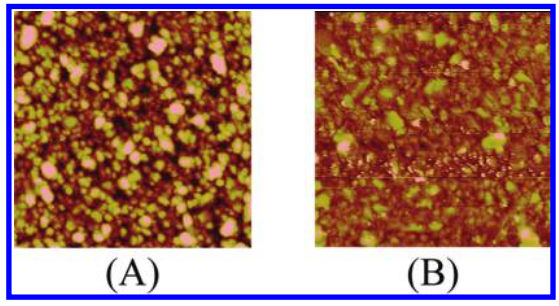

Figure 2. AFM images of silver-sputtered QCM crystals ($3 \times 3\ \mu m^2$ with Z range of 15 mm) (A) Ag-polished crystal without sugar film (blank); (B) Ag-polished crystal with Ac-β-GLU film (coated).

derivatives using the QCM technique. Five sugar acetates were selected (Figure 1), together with two primitive sugars α-GLU and α-CD as a comparison. These sugar acetates were Ac-α-GLU, Ac-α-GAL, Ac-β-GLU, SOA, and Ac-β-CD, differing with each other in chemical structure and number of acetyl groups. In particular, Ac-α-GLU and Ac-β-GLU are anomers with the only structural difference being whether the acetate substituent is equatorial or axial on the anomeric carbon. In the case of the Ac-α-GLU and Ac-α-GAL, which are epimers, the only difference is the configuration of the acetate on the C4 carbon (equatorial versus axial). SOA is a disaccharide consisting of fructose and glucose rings bonded through the anomeric carbon of the α-glucose, and Ac-β-CD consists of seven β-glucose rings connected in a 1,4-linkage with a total of 21 acetates per cyclodextrin molecule.

4.1. Influence of Surface Roughness on the Accuracy of Absorption Measurement. Since the frequency of a QCM crystal exposed to high pressure fluid is possibly affected by the surface roughness of the film on the crystal it is critical to evaluate the extent of the influence. The AFM technique was applied initially to determine the surface roughness of the crystal with and without a sugar coating and two typical AFM images of silver-sputtered crystals are shown in Figure 2. The rms (root-mean-square) surface roughness of the blank crystal (Figure 2A) was determined to be 3.7 nm whereas that of the coated crystal with Ac-β-GLU (Figure 2B) was 7.3 nm. In addition, it was found that the rms surface roughness of all coated crystals with different masses of Ac-β-GLU or sugar derivatives were less than 10 nm. The difference in surface roughness between the uncoated and coated crystals in Figure 2 is so little that the frequency shift caused by surface roughness can be regarded as negligible in comparison with the film mass contribution. This can be further verified from the determination of CO_2 absorption in SOA, as exemplified in Figure 3 and 4.

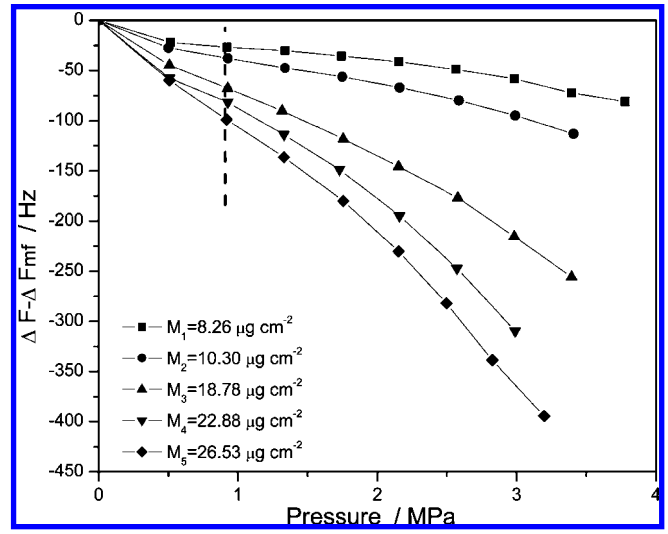

Figure 3. Plots of frequency change at 313.15 K as a function of CO_2 pressure for SOA films of different masses.

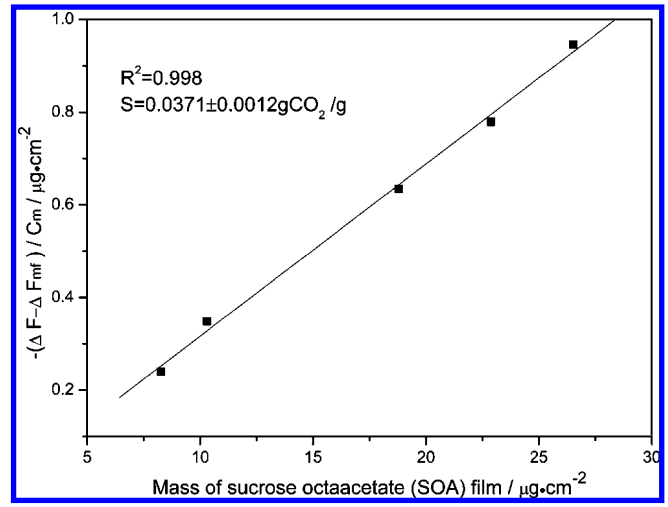

Figure 4. Plot of frequency change as a function of mass of SOA films coated on crystal electrode at 313.15 K and 1.0 MPa, indicating the determination of CO_2 absorption.

A series of plots of $(\Delta F - \Delta F_{mf})$ with respect to the mass of SOA film as a function of pressure are shown in Figure 3. It is evident that the value of $(\Delta F - \Delta F_{mf})$ decreases with the increasing sugar mass and pressure. The absorption of CO_2 in the sugar film was obtained from the slope of the linear plots of $-((\Delta F - \Delta F_{mf}))/(C_m)$ against the sugar mass at a given temperature and pressure of CO_2 (i.e., at 313.15 K and 1.0 MPa as shown from the dashed line in Figure 3). The correlation coefficient of the plot (see Figure 4) is found to be better than 0.998, and the relevant deviation of CO_2 absorption is around 3.0%. In the cases of other pressures, temperatures, or sugar acetates, the same procedure of absorption measurement was applied and most the plots of $-((\Delta F - \Delta F_{mf}))/(C_m)$ vs film mass (M) show good linearity with correlation coefficients more than 0.995 and the resulting relative deviations of CO_2 absorption less than 5%. It is clearly shown from Figure 3 and 4 that the surface roughness contribution to the frequency shift, ΔF_r, was canceled out by plotting $-((\Delta F - \Delta F_{mf}))/(C_m)$ against film

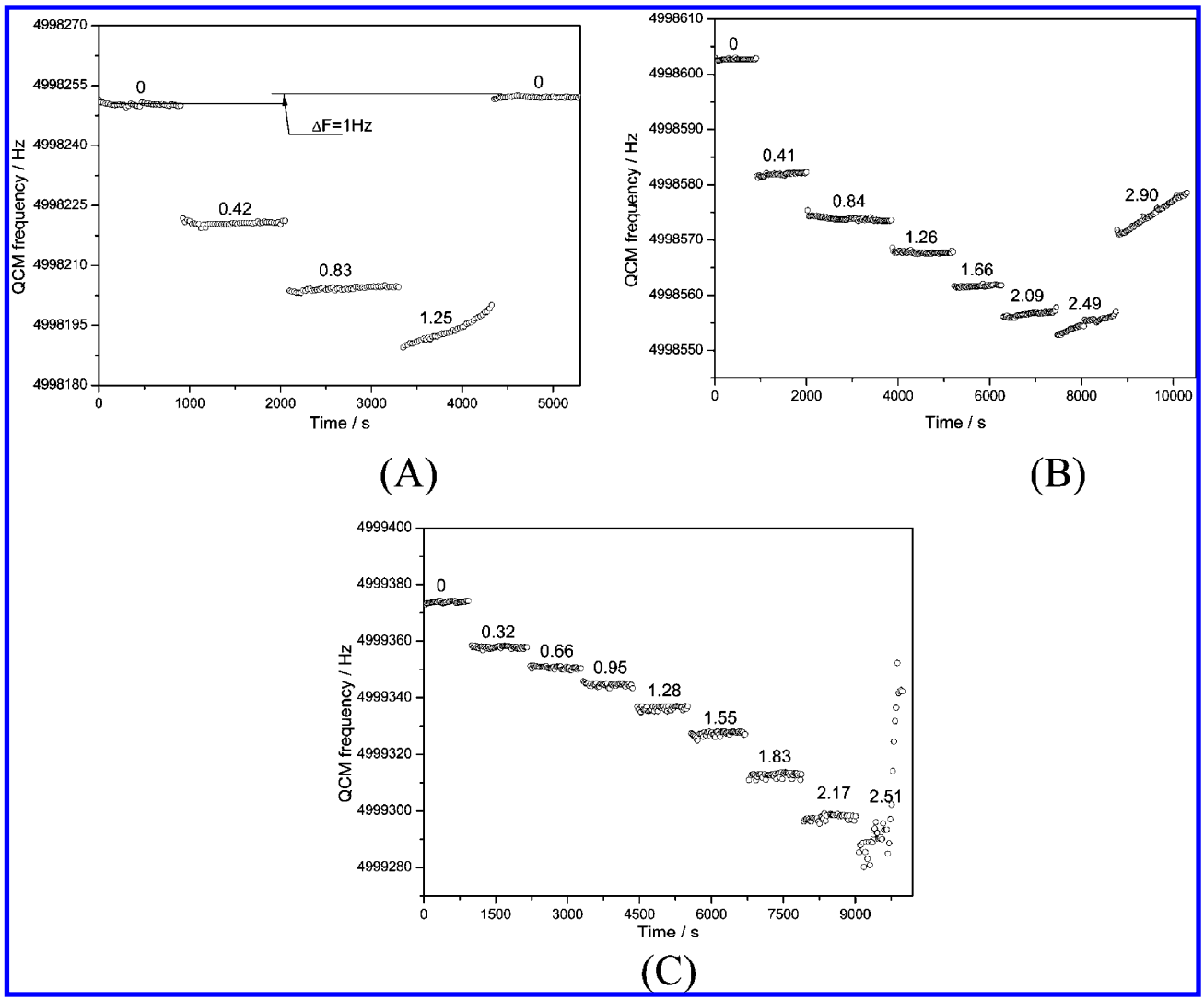

Figure 5. Plots of QCM frequency at different pressures of CO_2 versus time for different sugar acetate coatings, showing the occurrence of deliquescence. The numbers above the plots are pressure values in MPa. (A) Ac-α-GLU with 7.1 $\mu g \cdot cm^2$ coating at 293.15 K; (B) Ac-α-GLU with 3.9 $\mu g \cdot cm^2$ coating at 293.15 K; (C) Ac-α-GLU with 7.4 $\mu g \cdot cm^2$ coating at 313.15 K.

mass, and the CO_2 absorption measurement method established in the study is very feasible and precise.

4.2. Influence of Deliquescence on the Measurement. Previous studies have reported some visual observations of CO_2-induced deliquescence of carbohydrates,[5,35] and the deliquescence point at which solid−liquid−gas three phase equilibrium occurs in the global phase behavior of CO_2-sugar acetate mixture.[5,35] However, few efforts are seen to explore the influencing factors of CO_2-inducing deliquescence in the sugar acetates. In this study, the QCM technique was used to allow for the potential examination of such deliquescence phenomenon. Plots of QCM frequency at different pressures of CO_2 versus time for different sugar acetate coatings are shown in Figure 5A−C, and the deliquescence pressure of several sugar acetates at evaluated temperatures are summarized in Table 1.

As shown in Figure 5A, the QCM frequency F for the Ac-α-GLU film decreased with increasing pressure and reached a steady state (the frequency change observed to within ±1 Hz over 15 min) and defines the dissolution equilibrium at the given pressure. However, when the pressure was increased to 1.25 MPa, the QCM frequency initially decreased owing to CO_2 loading then began to increase gradually and could not maintain a stable frequency. Since the CO_2 loading in chemical films increases with pressure and induces a decrease in the QCM frequency, the unexpected increasing frequency observed at 1.25 MPa in Figure 5A was ascribed to the deliquescence of Ac-α-GLU. This was interpreted as the phase transition of the original

TABLE 1: Deliquescence Pressures of Sugar Acetates at Evaluated Temperatures

sugar acetates	T/K	deliquescence pressure/MPa	corresponding film mass/$\mu g \cdot cm^{-2}$
SOA	273.15	~2.8	3.0
	273.15	~2.6	6.6
	293.15	>4.2[a]	5.1
	313.15	>4.1[a]	9.8
	333.15	~4.7	9.1
	333.15	~4.2	13.1
Ac-α-GLU	293.15	~2.5	3.9
	293.15	~1.2	7.1
	313.15	~2.5	7.4
Ac-α-GAL	313.15	~2.4	8.0
Ac-β-GLU	313.15	~4.0	5.6
Ac-β-CD	313.15	>6.0[a]	8.2

[a] Deliquescence was not detected within the experimental pressure range.

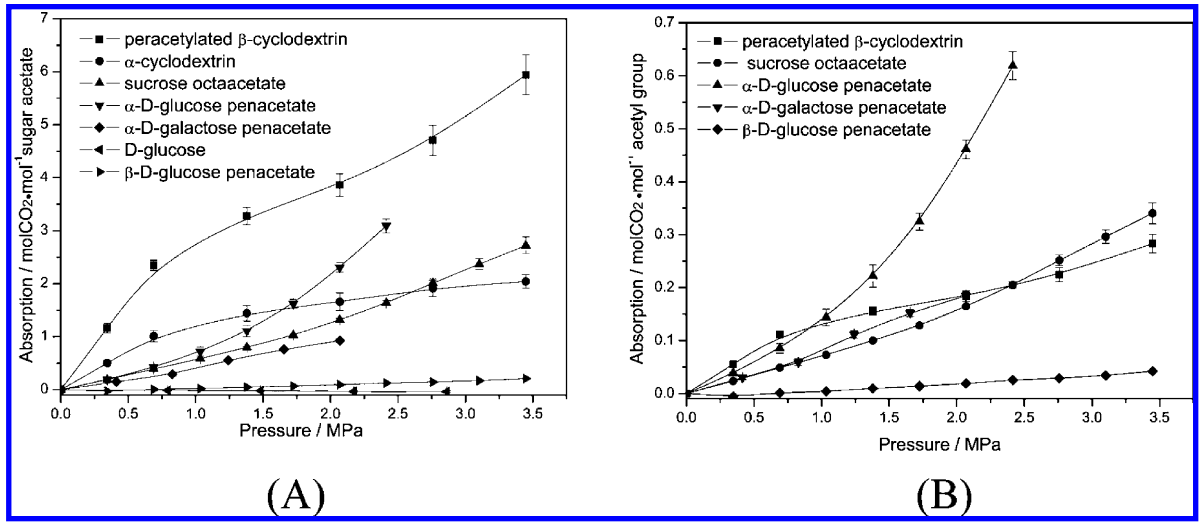

Figure 6. Absorption of CO_2 in different sugar derivatives at 313.15 K as a function of CO_2 pressure. (A) Absorption of CO_2 in the unit of mole CO_2 per mole sugar acetate; (B) absorption of CO_2 in the unit of mole CO_2 per mole acetyl group.

solid sugar acetate film undergoing liquefaction in contact with gaseous CO_2. It is believed that the sugar acetate remains on the QCM surface when the pressure is raised to higher values since the compound did not dissolve in the gaseous CO_2 environment. This is illustrated by the fact that the QCM frequency returned to the original value of the solid film at the vacuum condition after the CO_2 pressurization-depressurization cycle (see Figure 5A).

Once deliquescence occurs, the absorption equilibrium can not be reached due to continuously increasing CO_2 mass during the phase transition. Moreover, the frequency change determined is not in accordance with the mass calculated from the Sauerbrey equation. This is because only very thin liquefied films can be approximated as rigid to satisfy the assumption in the Sauerbrey equation. Additionally, variations in density and viscosity of the liquid film, known as the viscoelasticity effect,[36−38] can induce additional frequency responses.

Since the mass of the sugar acetate coating on the QCM crystal has a linear relationship with the thickness of sugar film, the measured deliquescence pressure was found to depend on the mass of sugar acetate. For example, the QCM frequency was able to reach equilibrium values at pressures up to 2.1 MPa when the Ac-α-GLU coating changed its mass value from 7.1 to 3.9 $\mu g \cdot cm^{-2}$ (see Figure 5A,B); whereas the measured deliquescence pressure of SOA at 313.15 K decreased from 4.7 to 4.2 MPa when the film mass of SOA increased from 9.1 to 13.1 $\mu g \cdot cm^{-2}$ (see Table 1). Thick films are easily softened after absorbing enough CO_2, leading to the viscoelasticity effect on the QCM frequency as well as the decrease of the measured deliquescence pressure. Therefore, the measurement of deliquescence pressure using thin films is more accurate than using thick films.

Temperature is another factor that influences the deliquescence of sugar acetates. It is evident from Figure 5C that the deliquescence pressure for the Ac-α-GLU film at 293.15 K was as low as 1.25 MPa, less than the data at 313.15 K (about 2.51 MPa). The experimental data presented in Table 1 also reveals that the deliquescence pressure for SOA increases gradually when the temperature rises from 273.15 to 333.15 K. This may be due to the decreasing molecular interaction strength of CO_2 with SOA at elevated temperatures.

It should also be mentioned that although the film thickness of sugar acetate coatings were similar and the temperature was fixed at 313.15 K the deliquescence pressure for various sugar acetates was quite different (see Table 1). For example, Ac-β-GLU begins deliquescence at 4.0 MPa, much higher than Ac-α-GAL (2.4 MPa) and Ac-α-GLU (2.5 MPa) at 313.15 K, and the deliquescence of Ac-β-CD was not been experimentally detected when the pressure was as high as 6.0 MPa at the same temperature. In this case, the influence of molecular structure of sugar acetates should be taken into account. Theoretically, all the variations in the molecular structure of sugar acetates including configuration, molecular size, as well as number of acetyl groups would have had a certain influence on the interaction between sugar acetates and CO_2, resulting in different deliquescence pressures for various sugar acetates.

To our knowledge, this is the first time in situ quantitative measurement of a CO_2-induced phase transition for sugar acetates using a microbalance technique. The ease and reproducibility of the QCM technique makes it a valuable addition to the tools available to study CO_2-induced phase transitions in organic films. All the CO_2 absorption presented in the following text were recorded using pressures lower than deliquescence pressure of each sugar derivative.

4.3. Effects of Molecular Structure and Acetyl Content on CO_2 Absorption. The absorption of CO_2 in five sugar acetates, as well as in two primitive sugars D-glucose and α-CD were measured at 313.15 K and pressures up to 4.0 MPa, as shown in Figure 6. In addition, SOA was chosen as an example to investigate the temperature dependence of CO_2 absorption. The CO_2 absorption data at elevated pressures up to 4.0 MPa and temperatures ranging from 273.15 to 333.15 K are available in Figure 7.

As shown in Figure 6A, compared to nearly no CO_2 absorption in the primitive sugar α-glucose, its peracetylated derivative, Ac-α-GLU exhibited a significant amount of CO_2 absorption, confirming the existence of attractive interactions between CO_2 and the acetyl groups of sugar acetates. The affinity results from the Lewis acid−Lewis base interactions between the carbon atom of CO_2 and the oxygen atom in the acetyl group, together with the weak hydrogen bond interaction of C−H···O between the oxygen atom of CO_2 and the hydrogen atom in the acetyl group, as demonstrated in the literature.[5,8,9] These two oriented interactions act cooperatively and become the direct reason of good CO_2 absorption.

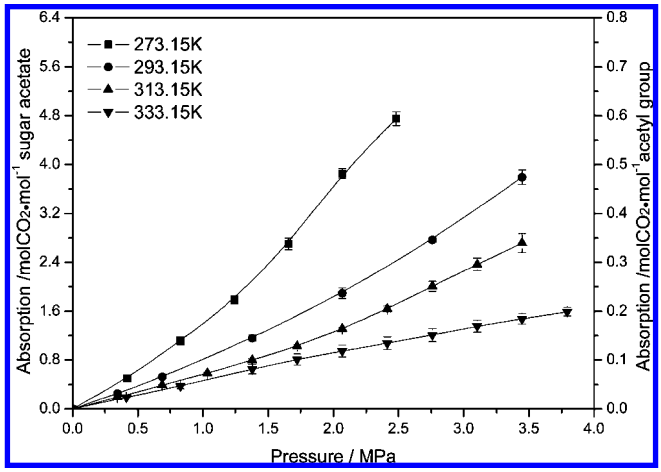

Figure 7. Absorption of CO_2 in SOA as a function of CO_2 pressure and temperature.

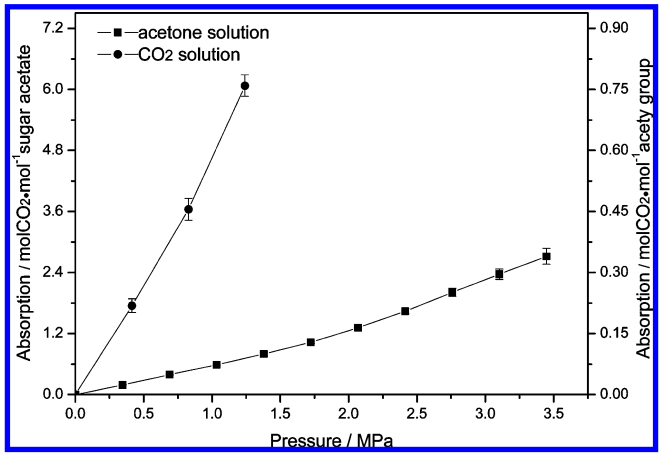

Figure 8. The effect of long-range order on the supercritical CO_2 absorption properties of SOA films at 313.15 K.

Theoretically, it would be expected that one CO_2 molecule would interact with each acetyl group giving a 1:1 complex. However, in the present study this is unlikely due to structural differences in the sugars studied in which the number of inter- and intramolecular contacts of the acetyl carbonyls reduce the number of interaction sites available for CO_2. Nevertheless, the quantity of CO_2 absorbed into this simple sugar acetate (Ac-α-GLU) film reaches 0.6 mol/mol acetyl group at 2.5 MPa and is quite high (Figure 6B).

Sugar acetate-CO_2 systems are found to have different cloud points based on their chemical structure.[5] In this study, a series of pentaacetylated sugars, Ac-α-GLU, Ac-α-GAL, and Ac-β-GLU were chosen for the quantitative investigation of the influence of crystal structure and spatial conformation of sugar molecules on CO_2 absorption. These sugars are all structural isomers of one another, that is, Ac-α-GLU and Ac-α-GAL are epimers while Ac-α-GLU and Ac-β-GLU are anomers. However, their capacity of CO_2 absorption is quite different, that is, the CO_2 absorption in Ac-α-GLU is almost 25 times higher than Ac-β-GLU at about 2.5 MPa (Figure 6A). The crystal structure of sugar acetates reveal that there also exists C−H···O interactions between acetyl groups in the lattice, and the nature of CO_2 dissolution in sugar acetates is determined by the interand intramolecular interactions between acetyl groups in sugar acetate, along with their interaction with CO_2.[5] For Ac-β-GLU, all the five acetyl groups are in the equatorial position and such spatial conformation is very stable, leading to a strong interaction between acetyl groups in the crystal structure. This hypothesis is made stronger by the high melting point of Ac-β-GLU (405 K, Ac-α-GLU 382K), revealing that the lattice energy of Ac-β-GLU is large. Therefore, the fact that the CO_2 absorption in Ac-β-GLU is much less than Ac-α-GLU could primarily be due to the strong intramolecular interaction between acetyl groups in Ac-β-GLU crystal.

Experimental results also indicate that there is a significant difference in the CO_2 absorption between the glucose and galactose epimers, that is, Ac-α-GAL adsorbed approximately one-third the amount the GLU epimer does at 2.1 MPa (Figure 6A). In the spatial conformation of Ac-α-GAL, a strong repulsion between acetyl groups on the anomeric and C4 carbon might exist since both are axial. Therefore it is posulated that once a C−H···O interaction is formed between a CO_2 molecule and one of these two acetyl groups, the other acetyl group is inaccessible to CO_2 because of the stereohindrance effect. Thus the number of interaction sites for CO_2 is reduced, resulting in a smaller CO_2 absorption.

The molecular size of sugar acetates and the quantity of acetyl moieties are thought to have an influence on the CO_2 absorption capacity. To test this, CO_2 absorption of SOA, Ac-β-CD, and Ac-α-GLU were compared. By plotting the CO_2 absorption in units of mole CO_2 per mole of acetyl group when the CO_2 pressure exceeded 2.5 MPa (Figure 6B), the CO_2 absorption showed a general trend of decreasing with increasing molecular weight and number of acetyl groups (Ac-α-GLU > SOA > Ac-β-CD). This result suggested that although the CO_2-acetyl interaction is important to the absorption of CO_2, it is crucial to consider the geometric packing of the sugar and the overall accessibility of the acetyl groups in these systems. Since SOA and Ac-β-CD have a larger molecular size and more acetyl groups than Ac-α-GLU, the spatial resistance between acetyl groups in the crystal structure maybe increase accordingly, reducing the number of effective interaction sites for CO_2. When the CO_2 pressure is lower than 2.5 MPa, Ac-β-CD seemed to absorb CO_2 more availably than SOA, which could be attributed to the additional chemical inclusion of CO_2 into the cage of Ac-β-CD (Figure 6B). This is demonstrated by comparing the CO_2 absorptions in two primitive sugars, α-cyclodextrin and α-glucose. Figure 6A shows that α-cyclodextrin exhibited high CO_2 absorption even at low pressures (<1.5 MPa), and the absorption reached a limit at high pressures (>2.0 MPa), suggesting the existence of saturated CO_2 absorption. This behavior is primarily due to chemical absorption and could be ascribed to the structural cavity of α-CD molecule trapping CO_2 molecules. Since Ac-β-CD has both acetyl groups and a cavity it is thought that absorption of CO_2 is due to a combination of both physical and chemical interactions, exhibiting the highest CO_2 absorption among the sugar acetates tested (Figure 6A). The absorption profile of CO_2 for Ac-β-CD shows a stretched "S" curve with a reflection point located around 1.5 MPa. The reflection point is thought to be a representation of the end of either the chemical or physical dominated absorption.

The solubility of CO_2 in sugar acetates without cage structures such as Ac-α-GLU, Ac-α-GAL, Ac-β-GLU, and SOA were found to increase almost linearly with the increasing pressure (especially when the pressure was lower than 1.5 MPa as shown in Figure 6A). This makes sense if the pressure effects on the absorption are attributable to the strength of the intermolecular interactions, which would decrease gradually with the increasing temperature due to

the reduced CO_2 density (see Figure 7). These are typical and characteristic phenomena of physical absorption. Later, some thermodynamic parameters such as Henry's law constant and enthalpy and entropy of CO_2 dissolution of these sugar acetates are calculated to evaluate the physical interactions of the sugar acetate with CO_2.

Previous studies using sum frequency generation (SFG) spectroscopy and differential scanning calorimetry (DSC) established that some carbohydrates such as SOA and Ac-β-CD become amorphous when they are precipitated from liquid CO_2.[11] Since coated films precipitated from organic solvents remain crystalline,[34] the effect of the coating method and the structural order of the carbohydrate film on the CO_2 absorption were also considered. In Figure 8, the CO_2 absorption is presented as a function of CO_2 pressure for SOA coated from an acetone and a CO_2 solution at 313.15 K. There is a striking difference in the absorption of CO_2 for the two kinds of films. It was found that the amorphous film was able to absorb significantly higher quantities of CO_2 compared to the crystalline film. The results can be explained in terms of the packing arguments discussed previously and the nature of inter- and intramolecular C−H···O contacts in the molecular structure of SOA. During dissolution of sugar acetates in CO_2 solution, the C−H···O interaction present in the crystalline material is disrupted and replaced by the "CO_2-philic" C−H···O contacts. When the CO_2 is vented, the interaction between acetyl groups cannot be recovered, generating an amorphous structure. The lack of long-range order in such amorphous system allows more degrees of freedom for the acetyl groups to interact with CO_2 and leads to the increasing accessibility of CO_2 to the acetate groups so that the CO_2 absorption increases dramatically.

4.4. Thermodynamic Analysis of the Interactions between Acetyl Group and CO_2. For the physical absorption of CO_2 in a sugar acetate, the equilibrium concentration (absorption capacity) of pure CO_2 in the sugar acetate can be described using the extended Henry's law[16]

$$f = P\varphi = k_H(T)\exp\left(\frac{V^\infty P}{RT}\right)x\gamma^* \tag{9}$$

where f and ϕ are the fugacity and fugacity coefficient of CO_2 in the vapor phase, respectively. $k_H(T)$ is the Henry's constant of CO_2 in the sugar acetate when the CO_2 pressure approaches zero, being only a function of temperature. V^∞ is the partial molar volume of CO_2 at infinite dilution, x is the molar fraction (equilibrium concentration) of CO_2, and γ^* is the normalized activity coefficient of CO_2 in the sugar acetate that is dependent on x. By limiting the pressure P in eq 9 to zero, $k_H(T)$ can be obtained from experimental absorption data as

$$k_H(T) = \lim_{P\to 0}\frac{f}{x} \approx \frac{P}{x} \tag{10}$$

The approximations in eq 10 holds since both the fugacity and activity coefficients ϕ and γ^* in eq 8 are of unity when P approaches zero, and eq 10 reduced from eq 8 becomes Henry's law accordingly. However, due to the high CO_2 absorption γ^* is nonideal and the Henry's constant $k_H(T)$ has to be determined by fitting a second-order polynomial to the experimental absorption data and calculating the limiting slope as the pressure approaches zero.[14,39]

The knowledge of Henry's constant of CO_2 in sugar acetates allows for the calculation of further solution thermodynamic properties, by applying the following thermodynamic relationships[16]

$$\Delta_{sol}G = RT\ln(k_H(T,P)/P^0) \tag{11}$$

$$\Delta_{sol}H = R\left(\frac{\partial \ln(k_H(T,P)/P^0)}{\partial(1/T)}\right)_P \tag{12}$$

$$\Delta_{sol}S = (\Delta_{sol}H - \Delta_{sol}G)/T \tag{13}$$

where $\Delta_{sol}G$, $\Delta_{sol}H$, $\Delta_{sol}S$ are the partial molar Gibbs energy, enthalpy, and entropy of CO_2 absorption in a sugar acetate, respectively. The thermodynamic analysis of the absorption data can provide theoretical insight into the interactions between CO_2 and the acetyl group in sugar acetates.

The Henry's constants, enthalpy, and entropy calculated from the absorption experiments presented above are listed in Table 2, together with these thermodynamic values for CO_2 in three typical ionic liquids (ILs)[15,16,40] for comparison. Ionic liquids, with good CO_2 absorption capacity and favorable properties,[15,16] such as nonflammability and negligible vapor pressure, have received extensive attention in separating CO_2 from a wide variety of gas sources.[15] Generally, sugar acetates tested in this work are found to have smaller values of Henry's constant than the ILs, indicating that sugar acetates are better CO_2 absorbers. In addition, the enthalpy and entropy of dissolution for CO_2 in SOA are in the same order of magnitude with ILs, which suggests that the absorption behavior of CO_2 in these materials are both exothermic and the interactions of CO_2 with sugar acetates are quite similar to that of ILs.

It should also be mentioned that the total pressure of industrial gas sources such as natural gas, flue gas, water gas, and various prepared fuel gases is usually no more than 3 MPa, and the corresponding CO_2 mass fraction is less than 15%. To our knowledge, the deliquescence of sugar acetate is mainly due to the partial pressure of CO_2, and sugar acetates would not undergo deliquescence at such low partial pressures of CO_2 during the separation of CO_2. In fact, even though the CO_2 isolation has to be operated at partial pressures higher than the deliquescence point, the liquefaction of sugar acetates may still benefit to the process since the diffusivity of CO_2 into liquid is much higher than into solid. Because of this and other environmentally benign features, sugar acetates are believed to have the potential as the green mediums of CO_2-separation and other CO_2-involving processes.

5. Conclusions

In the present study the QCM technique has been successfully applied to determine the absorption of CO_2 into several sugar derivatives at temperatures from 273.15 to 333.15 K and pressures up to 4.0 MPa. The technique was demonstrated to be a simple, sensitive, and accurate tool for the measurement of gas absorption, especially under high pressure conditions. In addition, it was shown to be sensitive to the changes in the physical makeup of the surface films, which was determined to be a phase transformation from a solid to a liquid film, also known as a deliquescence point. To date this is the first in situ demonstration of a CO_2 induced phase change detected with quantitative precision using a QCM.

TABLE 2: Henry's Constant of CO_2 in Sugar Acetates and Ionic Liquids

sugar derivatives	T/K	k_H/MPa	Enthalpy[a]/ kJ·mol^{-1}	Entropy[a]/ J·mol^{-1}
SOA	273.15	1.35 ± 0.07	−10.2	−59.8
	293.15	2.02 ± 0.09		
	313.15	2.52 ± 0.07		
	333.15	2.94 ± 0.08		
Ac-α-GLU	313.15	2.10 ± 0.01	n.a.[b]	n.a.[b]
Ac-α-D-GAL	313.15	2.94 ± 0.15	n.a.[b]	n.a.[b]
[bmim][BF_4][15]	313.15	7.51[c]	−15.9	−52.4
[bmim][PF_6][16]	313.15	8.52 ± 0.21[d]	−17.2	−79.5
[bmim] [Tf_2N][40]	313.2	6.41 ± 0.18[d]	n.a.[b]	n.a.[b]

[a] Calculated at the standard temperature and pressure (T^0 = 298.15 K, P^0 = 0.1 MPa). [b] n.a. = not available. [c] Interpolated value from the data in ref 15.

It was also the first time that QCM was used to evaluate the effects of various structural changes in sugar derivatives on high pressure CO_2 absorption. In general, sugar derivatives with accessible acetyl groups or cavities in the molecular structure were shown to have good CO_2 absorption, primarily due to the Lewis acid−Lewis base and hydrogen bond interactions between CO_2 and acetyl group, or the chemical inclusion of CO_2 into the cavity of cyclodextrin. In particular, the α anomer of Ac-GLU is shown to have an order of magnitude greater affinity for CO_2 binding relative to the β anomer since the latter has a much stronger C−H···O bond between acetyl groups in the crystal structure, whereas the epimers (α-GLU and GAL) exhibit a small difference in the CO_2 absorption. Ac-β-CD, having accessible acetyl groups and a cavity, was found to be the best CO_2 absorber especially at low pressures (<2.0 MPa). However, when the pressure exceeds 2.0 MPa, the CO_2 inclusion into the cavity becomes saturated, so that the physical interaction between CO_2 and acetyl groups dominates the absorption.

The QCM technique was also able to determine changes in the CO_2 absorption as a function of crystallinity. The long-range order of SOA was found to be destroyed by dissolving in high pressure CO_2, and the SOA film on the QCM electrode became amorphous by free meniscus coating in liquid CO_2 solution. The substantial increase of CO_2 absorption in the amorphous films over that in the crystalline films (cast from organic solution) was attributed to the increase in degrees of freedom and higher mobility in the absence of long-range order.

Generally speaking, the measurement of CO_2 absorption is of practical importance, and it is significant in the areas of solvation, development of more CO_2-philic materials and selection of better formulations for new CO_2-melt processing (i.e., pharmaceutical excipients and active reagents). In addition, since sugar acetates were comparable to ILs in absorbing CO_2 demonstrated from thermodynamic analysis of the CO_2 absorption data, and both of them are green materials for CO_2 absorption, it is believed that sugar acetates have a strong potential to be used in CO_2 separation.

Acknowledgment. This material is based upon work supported in part by the STC Program of the American National Science Foundation under Agreement No. CHE-9876674, the National Science Foundation of China under Agreement No. 20776065, the Science Foundation of Jiangsu province in China under Agreement No. 2008023, and the scientific research foundation of graduate school of Nanjing University. The authors would also like to gratefully acknowledge the assistance of the Krim and Carbonell research groups in addition to the Kenan Center at North Carolina State University for technical assistance and facility utilization.

References and Notes

(1) DeSimone, J. M. *Science* **2002**, *297*, 799.
(2) Hurtado-Benavides, A. M.; Señoráns, F. J.; Ibáñez, E.; Reglero, G. *J. Supercrit. Fluids* **2004**, *28*, 29.
(3) DÖker, O.; Salgin, U.; Sanal, I.; Mehmetoglu, U.; Calimli, A. *J. Supercrit. Fluids* **2004**, *28*, 11.
(4) Yaku, K.; Morishita, F. *J. Biochem. Biophys. Methods* **2000**, *43*, 59.
(5) Raveendran, P.; Wallen, S. L. *J. Am. Chem. Soc.* **2002**, *124*, 7274.
(6) Potluri, V. K.; Xu, J. H.; Enick, R. M.; Beckman, E.; Hamilton, A. D. *Org. Lett.* **2002**, *4*, 2333.
(7) Potluri, V. K.; Hamilton, A. D.; Karanikas, C. F.; Bane, S. E.; Xu, J. H.; Beckman, E. J.; Enick, R. M. *Fluid Phase Equilib.* **2003**, *211*, 211.
(8) Blatchford, M. A.; Raveendran, P.; Wallen, S. L. *J. Phys. Chem. A* **2003**, *107*, 10311.
(9) Raveendran, P.; Wallen, S. L. *J. Am. Chem. Soc.* **2002**, *124*, 12590.
(10) Fan, X.; Potluri, V. K.; McLeod, M. C.; Wang, Y.; Liu, J.; Enick, R. M.; Hamilton, A. D.; Roberts, C. B.; Johnson, J. K.; Beckman, E. J. *J. Am. Chem. Soc.* **2005**, *127*, 11754.
(11) Hurrey, M. L.; Wallen, S. L. *Langmuir* **2006**, *22*, 7324.
(12) Türk, M. G., U.; Steurenthaler, M.; Hussein, K.; Wahl, M. A. *J. Supercrit. Fluids* **2007**, *39*, 435.
(13) Raveendran, P.; Blatchford, M. A.; Hurrey, M. L.; White, P. S.; Wallen, S. L. *Green Chem.* **2005**, *75*, 129.
(14) Anthony, J. L.; Maginn, E. J.; Brennecke, J. F. *J. Phys. Chem. B* **2002**, *106*, 7315.
(15) Cadena, C.; Anthony, J. L.; Shah, J. K.; Morrow, T. I.; Brennecke, J. F.; Maginn, E. J. *J. Am. Chem. Soc.* **2004**, *126*, 5300.
(16) Perez-Salado Kamps, A.; Tuma, D.; Xia, J.; Maurer, G. *J. Chem. Eng. Data* **2003**, *48* (3), 746.
(17) Buttry, D. A.; Ward, M. D. *Chem. Rev.* **1992**, *92*, 1355.
(18) O'Sullivan, C. K.; Guilbault, G. G. *Biosens. Bioelectron.* **1999**, *14*, 663.
(19) Thompson, M.; Kipling, A. L.; Duncan-Hewitt, W. C.; Rajakovic, L. V.; Cavic-Vlasak, B. A. *Analyst* **1991**, *116*, 881.
(20) Ward, M. D.; Buttry, D. A. *Science* **1990**, *249*, 1000.
(21) Park, K.; Koh, M.; Yoon, C.; Kim, H. *J. Supercrit. Fluids* **2004**, *29*, 203.
(22) Sato, Y.; Takikawa, T.; Takishima, S.; Masuoka, H. *J. Supercrit. Fluids* **2001**, *19*, 187.
(23) Aubert, J. H. *J. Supercrit. Fluids* **1998**, *11*, 163.
(24) Miura, K.-i.; Otake, K.; Kurosawa, S.; Sako, T.; Sugeta, T.; Nakane, T.; Sato, M.; Tsuji, T.; Hiaki, T.; Hongo, M. *Fluid Phase Equilib.* **1998**, *144*, 181.
(25) Abbott, A. P.; Brooks, N.; Eltringham, W.; Hillman, A. R.; Hope, E. G. *J. Polym. Sci., Part B: Polym. Phys.* **2006**, *44*, 1072.
(26) Pantoula, M.; Panayiotou, C. *J. Supercrit. Fluids* **2006**, *37*, 254.
(27) Nakamura, K.; Hoshino, T.; Suzuki, Y.; Yosizawa, H. *Dev. Food Eng., Proc. Int. Congr. Eng. Food, 6th* **1994**, 823.
(28) Guigard, S. E.; Hayward, G. L.; Zytner, R. G.; Stiver, W. H. *Fluid Phase Equilib.* **2001**, *187−188*, 233.
(29) Sauerbrey, G. *Z. Phys.* **1959**, *155*, 206.
(30) Tsionsky, V.; Daikhin, L.; Urbakh, M.; Gileadi, E. *Langmuir* **1995**, *11*, 674.
(31) Wu, Y. T.; Akoto-Ampaw, P. J.; Elbaccouch, M.; Hurrey, M. L.; Wallen, S. L.; Grant, C. S. *Langmuir* **2004**, *20*, 3665.
(32) Daikhin, L.; Urbakh, M. *Langmuir* **1996**, *12*, 6354.
(33) Urbakh, M.; Daikhin, L. *Langmuir* **1994**, *10*, 2836.
(34) Novick, B. J.; DeSimone, J. M.; Carbonell, R. G. *Ind. Eng. Chem. Res.* **2004**, *43*, 515.
(35) Hong, L.; Thies, M. C.; Enick, R. A. *J. Supercrit. Fluids* **2005**, *34*, 11.
(36) Banda, L.; Alcoutlabi, M.; McKenna, G. B. *J. Polym. Sci., Part B: Polym. Phys.* **2006**, *44*, 801.
(37) Carla, V.; Wang, K.; Hussain, Y.; Efimenko, K.; Genzer, J.; Grant, C.; Sarti, G. C.; Carbonell, R. G.; Doghieri, F. *Macromolecules* **2005**, *38*, 10299.
(38) Hussain, Y.; Wu, Y. T.; Ampaw, P. J.; Grant, C. S. *J. Supercrit. Fluids* **2007**, *42*, 255.
(39) Anthony, J. L.; Anderson, J. L.; Maginn, E. J.; Brennecke, J. F. *J. Phys. Chem. B* **2005**, *109*, 6366.
(40) Aki, S. N. V. K.; Mellein, B. R.; Saurer, E. M.; Brennecke, J. F. *J. Phys. Chem. B* **2004**, *108*, 20355.

JP9122634